Modelling of vertical piles subjected to a clay crust movement over a liquefied soil

Ripon Karmaker & Bipul Hawlader
Memorial University of Newfoundland, St. John's, NL, Canada
Sujan Dutta
Terraprobe, Brampton, ON, Canada

ABSTRACT
Piles might be subjected to passive loading from permanent ground deformations. The present study investigates the lateral force on a pile resulting from a downslope displacement of a clay crust over a liquefied soil layer. Finite-element (FE) analyses are performed to calculate the total force and its variation with depth in the segment of the pile in the crust. Analyses are performed for a single row of piles with a varying centre-to-centre spacing and undrained shear strength of clay. The FE results show that the pile behaves as a single pile when the spacing is greater than five times its diameter. The arching effects in relation to pile spacing are discussed. The lateral force per pile decreases with a decrease in pile spacing. Using the calculated maximum lateral force, a separate analysis is performed to examine the structural response of a long pile installed through the liquefied layer on a stable soil layer.

RÉSUMÉ
Les piles pourraient être soumises à une charge passive due à des déformations permanentes du sol. La présente étude étudie la force latérale sur une pile résultant d'un déplacement en pente d'une croûte d'argile sur une couche de sol liquéfié. Des analyses par éléments finis (EF) sont effectuées pour calculer la force totale et sa variation avec la profondeur dans le segment de la pile dans la croûte. Les analyses sont effectuées pour une seule rangée de piles avec un espacement centre-centre et une résistance au cisaillement non drainé variable de l'argile. Les résultats FE montrent que la pile se comporte comme une seule pile lorsque l'espacement est supérieur à cinq fois son diamètre. Les effets d'arche en relation avec l'espacement des poils sont discutés. La force latérale par pile diminue avec une diminution de l'espacement des poils. En utilisant la force latérale maximale calculée, une analyse séparée est effectuée pour examiner la réponse structurale d'un long pieu installé à travers la couche liquéfiée sur une couche de sol stable.

1 INTRODUCTION

Piles can be subjected to two different types of lateral loads. In active pile loadings, the lateral forces, which might come from superstructures, create a load on the pile and then transfer to the surrounding soil through pile–soil interaction. In this case, the soil surrounding the pile provides a resistance to the movement of the pile. In passive piles, the displacement of a layer/block of soil near the ground surface creates a load on the pile, which is then transferred to the deeper soil layers through pile–soil interaction.

The ground deformation could be caused by slope failure, lateral spreading due to the formation of a weak failure plane or liquefaction of loose sand layer(s) due to an earthquake. In many cases, a non-liquefied soil layer above the liquefied sand layer/weak zone displaces a significantly large distance, especially in a slopping ground condition, even for a mild slope. For example, Cubrinovski et al. (2009) reported permanent lateral ground displacements of up to 4 m in some mild-sloped areas after the 1995 Kobe earthquake. The displacement of soil caused significant damage to piles in those areas. The upper non-liquefied crust could be cohesionless, cohesive, or c-ϕ soil. The present study focuses on the estimation of lateral force that could be exerted on a pile due to downslope movement of a clay crust. As this type of ground deformation occurs quickly (e.g., during an earthquake or post-quake deformation), the soil is modelled for an undrained condition.

Physical and numerical modelling have been performed in the past to understand the response of piles in clay under active lateral loadings. For example, Welch and Reese (1972) and Matlock (1970) presented the response of instrumented piles under lateral loadings. Based on field test results, lateral load per unit length (p) versus displacement (y) curves have been developed to calculate the structural response of the pile. Centrifuge tests were also conducted to model the lateral pile–soil interaction (e.g., McVay et al. 1998 and Taghavi et al. 2016). Moreover, analytical solutions have been developed to calculate the maximum lateral resistance of clay on a section of the pile. For example, Randolph and Houlsby (1984) developed a closed-form solution for a single pile where the clay was modelled as an isotropic rigid-plastic Tresca material. The ultimate resistance has been presented in a normalized form as $N = P/s_uD$, where P is the lateral capacity per metre length of the pile, D is the diameter of the pile and s_u is the undrained shear strength of the clay. It has been shown that $N = 9.14$ and $N = 11.94$ for the fully smooth and perfectly rough pile–soil interface condition, respectively.

Empirical formulas, analytical solutions, and numerical techniques have been developed to calculate the passive load on vertical piles in clay. Conducting small-scale physical model tests, Bauer et al. (2014) showed a wide variation in the lateral force when a kaolin clay block interacts with a single pile or rows of piles. A summary of

available model tests and various recommendations for the estimation of the normalized lateral force is available in Bauer et al. (2014). Ito and Matsui (1975) developed an analytical approach to estimate the force on a pile installed in a row perpendicular to the ground movement. Some studies suggested the application of a free-field displacement to the sliding mass and calculation of the lateral force. In some studies, the Rankine passive earth pressure has been used to calculate the passive load on the pile (Cubrinovski et al. 2009). Three-dimensional FE analyses have also been performed to calculate the load on the pile on a sloping ground (Cai and Ugai 2000; Karmaker and Hawlader 2018). In these analyses, the "strength reduction" method is used to trigger the failure of the slope. Kourkoulis et al. (2012) proposed a hybrid decoupled approach for analysis and design of slope stabilizing piles. In their study, the lateral force needed to stabilize the slope has been calculated using three-dimensional FE simulations. Using this force, the optimum pile configuration has been identified from a decoupled analysis.

The downslope displacement of the crust layer in lateral spreading is expected to cause a large lateral force on the pile. In the present study, finite element simulation is performed first to calculate the lateral force exerted on the pile by a horizontally moving clay layer (crust), for a varying pile spacing and undrained shear strength of clay. The calculated force is then used for structural modelling of the pipeline, to present an example analysis.

2 PROBLEM STATEMENT

The problem analyzed in this study is shown schematically in Fig. 1. A row of long piles has been installed through varying soil composition to the stable layer. The ground surface has a mild slope. For simplicity, all the layers are assumed to be parallel to the ground surface. The unstable soil layer can lose the strength by the effects of natural factors (e.g., an earthquake) or by human activities (e.g., pile driving). This could cause a significant downslope movement of the upper crust (Cubrinovski et al. 2009).

For an earthquake, the ground movement does not necessarily occur only by the inertia force during the earthquake but under the gravitational load after the end of shaking. Kokusho (1999) showed that, if a loose sand layer is liquefied during an earthquake, the excess pore water pressure difference causes the flow of water towards the ground surface and might accumulate as a water film under the less permeable materials. Therefore, a water film might form below the clay crust, which could cause sliding of the crust of the idealized profile considered in this study. Note that free-field downslope displacements might also occur in the liquefied layer. However, these are not considered in this study. In other words, the downslope movement of only the crust is considered.

Based on field investigation after the 1995 Kobe earthquake, Cubrinovski et al. (2009) showed that the permanent lateral ground deformation caused the largest damage of the pile at two locations: the pile head and below the interface between the liquefied and stable soil layers. The force resulting from the movement of the crust was one of the main causes of this damage.

3 FINITE ELEMENT MODELING

The force generated by soil movements on the section of the pile in the crust is modelled using a 3-D FE modelling approach. A single row of circular piles of diameter *D* installed at a centre-to-centre spacing of *s* is modelled. Only the pile–soil interaction in the crust is modelled. As the slope is mild, the movement of the soil block is assumed to be horizontal over the interface between the clay crust and liquefied soil layer.

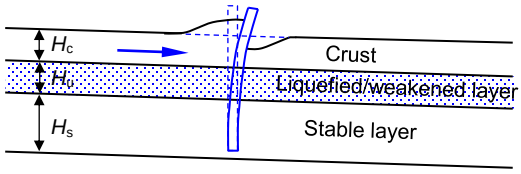

Figure 1. Downslope soil movement effects on pile

Figure 2 shows the three-dimensional FE model used in this study. Analysis is performed using Abaqus/Explicit FE software. A wished-in-place pile section (neglecting installation effects) in a 5.0 m thick crust of clay layer is modelled. The pile is 1.0 m above the initial ground surface, which is considered to model the accumulated soil behind the pile due to ground movement. The pile–soil interface behaviour is modelled as a fully bonded condition.

As the sliding could occur very quickly, the soil is modelled with undrained behaviour. Taking the advantage of symmetry, only half of the domain of thickness of s/2 is modelled. The left and right boundaries are placed at 10 m from the centre of the pile to avoid any boundary effects.

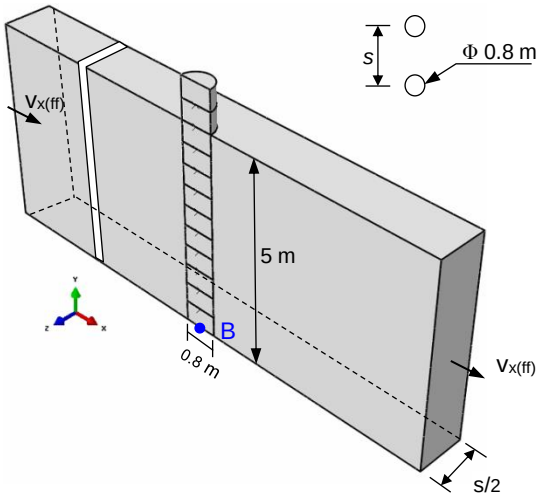

Figure 2: Problem definition

The pile is modelled as a rigid body. The authors understand that the flexibility of the pile could have an influence on the calculated force. The bottom surface of the domain is assumed to be smooth. No soil movement perpendicular to the faces of the domain is allowed, except for the left and right faces where a free-field

displacement—a lateral free-field velocity ($v_{x(ff)}$) of 0.01 m/s, is applied. As will be discussed in the later sections, the lateral instantaneous velocity of the soil elements (v_x) near the pile will be different from $v_{x(ff)}$.

The FE modelling consists of two loading steps. First, the gravity loading is applied gradually in 20 s. After that, the lateral displacement with $v_{x(ff)}$ = 0.01 m/s is applied over a period of 50 s. The automatic time increment, factored by 0.1, is used to avoid any numerical issues in the explicit analysis.

The numerical simulations are performed for D = 0.8 m and varying spacing of s = 2–8. For the first set of analyses, s_u = 40 kPa is used. The undrained Young's modulus (E_u) of 250s_u and undrained Poisson's ratio of 0.495 are used. A parametric study for varying s_u is also performed. The von Mises yield criterion is adopted.

4 RESULTS

4.1 Force–displacement behaviour

Figure 3 shows the variation of average normalized force ($N_{av} = F_x/(s_{uN}D_eL)$ with free-field displacement ($u_{x(ff)} = v_{x(ff)} \times t$, where t is the time during which the lateral velocity boundary conditions are applied). Here, D_e is the effective diameter and L is the total length of the pile (= 5 m). The total force on the pile (F_x) is twice the sum of the horizontal force on each rigid segment of the pile, as shown in Fig. 2. Note that the maximum force on a pile segment is smaller near the ground surface, increases with depth, and is almost constant after ~3 m. An effective diameter (D_e), instead of the outer diameter D_0 (= 0.8 m), is used to calculate the normalized force because a fully bonded condition is used. In this case, the failure occurs in the soil instead of sliding of soil at the pile–soil interface. Assuming that the failure occurs at the middle of the soil element next to the pile surface, $D_e = D_0 + t_{FE}$ = 0.8 + 0.1 = 0.9 m is calculated. Moreover, $s_{uN} = 2/\sqrt{3}s_u$, (please see Hawlader et al. 2015 for further discussion).

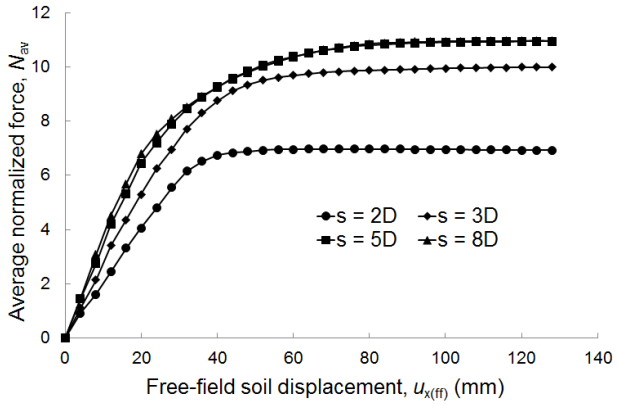

Figure 3: Variation of normalized force with free-field displacement

Figure 3 shows that N_{av} reaches the maximum value at a free-field displacement of approximately 40 to 80 mm; a larger displacement is required for a larger spacing. The maximum normalized force increases with pile spacing. The difference between the force–displacement curves for s = 5D and 8D is negligible, which indicates that the pile behaves as a single pile for the range of pile spacing.

The maximum normalized force for $s \geq 5D$ is approximately 10.5. As mentioned above, Randoloph and Houlsby (1984) calculated the maximum normalized forces of 11.94 and 9.14 for the rough and smooth pile–soil interface conditions, respectively.

4.2 Effects of pile spacing

The effects of pile spacing on the force–displacement behaviour, as shown in Fig. 3, are examined further, based on arching effects.

Figure 4 shows the contour of the horizontal component of the instantaneous velocity of soil elements (v_1) on a horizontal plane at a depth of 4.0 m below the original ground surface, for a free-field displacement of 100 mm. For the soil elements far from the pile, v_1 is approximately equal to the free-field velocity applied at the boundary (i.e., $v_1 = v_{x(ff)}$ = 0.01 m/s) for all four pile spacing cases. As expected, v_1 is very small near the pile. For s = 2D case, a large zone near the pile has a negligible velocity. Moreover, v_1 is very small up to the mid-distance between two piles because of arching effects (e.g., point A in Fig. 4(a)). Therefore, in this case, a considerable soil heave occurs in the left side of the pile for a large free-field displacement.

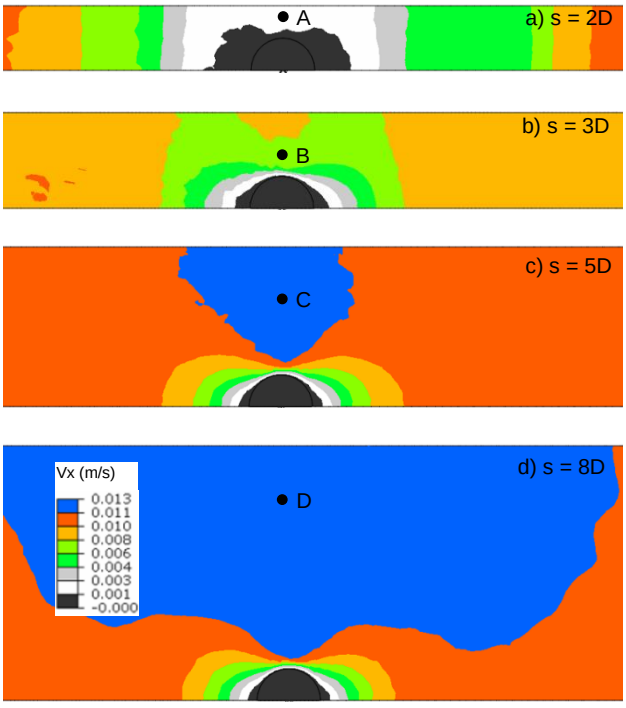

Figure 4: Instantaneous soil velocity at 4-m depth for 100-mm free-field displacement

For s = 3D, the tendency of soil to flow around the pile is higher than in s = 2D. Therefore, a higher v_1 is calculated near the pile (e.g., point B in Fig. 4(b)) than in s = 2D (e.g., point A). For s = 5 and s = 8, the arching effect is not sufficient to stop the soil flow between the piles. Therefore,

a higher velocity of soil elements near the pile (e.g., at points C and D in Figs. 4(c) and 4(d), respectively) is obtained, because the same amount of soil displaced in the free-field zone is passed through the narrower space between the piles.

4.3 Effects of undrained shear strength

The effects of undrained shear strength on force–displacement behaviour is examined by varying s_u between 10 and 40 kPa for s = 3D. As mentioned before, Young's modulus E_u = 250s_u is used. To show the effects of E_u, analyses are also performed for a constant E_u = 10 MPa.

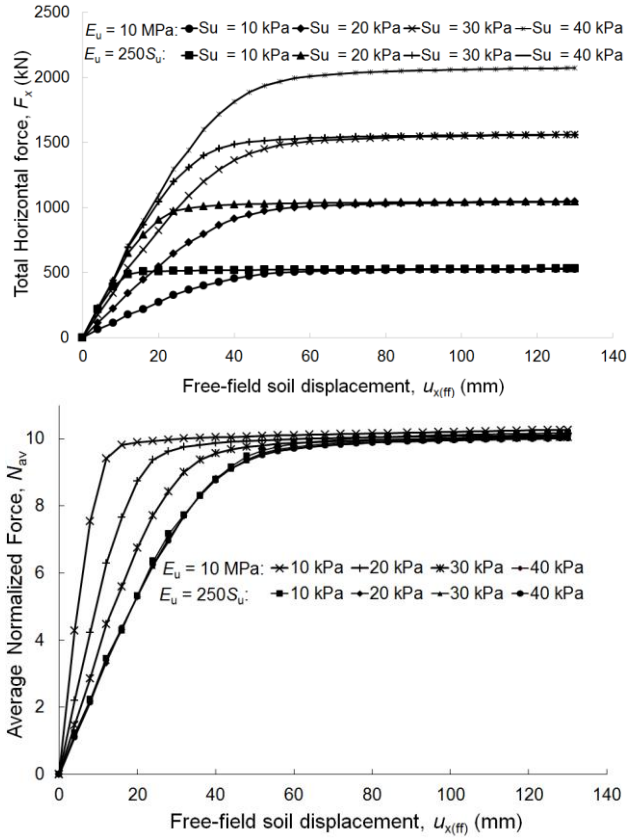

Figure 5: Effects of undrained shear strength and Young's modulus: (a) variation of horizontal force, (b) variation of average normalized force

Figure 5(a) shows the total lateral forces with free-field displacement. The maximum lateral force for a given s_u is the same for both E_u (E_u =10 MPa and 250s_u). However, the force–displacement curve prior to the mobilization of the maximum force is different—the higher the E_u, the faster the mobilization of force.

The normalized force–displacement curves (N_{av} vs. $u_{x(ff)}$) for these analyses are shown in Fig. 5(b). As shown, a single N_{av}–$u_{x(ff)}$ relationship is found when E_u = 250s_u is used; however, N_{av}–$u_{x(ff)}$ curves are different before the maximum N_{av} for the constant E_u. At a large free-field displacement, N_{av} is independent of s_u and E_u. Note that the maximum N_{av} will be smaller for closely spaced piles (e.g., s = 2D) that are shown in Fig. 5(b) (see also Fig. 3).

5 MODELLING OF STRUCTURAL RESPONSE–AN EXAMPLE

Consider a row of a 25-m long steel pipe pile of 0.8-m outer diameter and 45-mm wall thickness, which is installed in a three-layered soil, with a mild slope as shown in Fig. 1. The clay crust has a thickness (H_c) of 5 m and undrained shear strength (s_u) of 20 kPa. The thickness of the unstable loose sand layer (H_u) is 5 m. The shear strength of this soil layer is decreased due to an earthquake that caused sliding of the upper crust and permanent ground deformation. The groundwater table is assumed at the ground surface.

The structural response of the pile is calculated using LPile Version 8.03 software. For simplicity, only the bottom part of the pile (20 m) below the interface between the crust and liquefied layer is modelled. The authors understand that a fully coupled pile–soil interaction analysis could be performed using the FE technique presented above. However, this type of three-dimensional modelling with a flexible pile is computationally expensive, especially for a long pile and large centre-to-centre spacing. Moreover, the force from the clay crust could be presented better in the normalized form, as described above, and LPile is a widely used software in the industry; therefore, a decoupled analysis is performed for this paper.

The estimation of the lateral resistance of a liquefied soil layer is more difficult than for non-liquefied soils. As loose sand liquefies in an undrained condition, some studies modelled its behaviour as soft clay (Wang and Reese 1998). The residual shear strength, a constant or linear function of the initial vertical effective stress, is also used to estimate the maximum lateral resistance (Cubrinovski et al. 2009). The reduction of resistance using a "p-multiplier" of 0.1–0.3 was suggested in some studies (Liu and Dobry 1995; Wilson 1998). A conservative assumption of zero lateral resistance of liquefied soil is also available. Based on full-scale test results, Rollins et al. (2005) proposed a power function for the p–y curve, where p is the soil resistance and y is the lateral displacement, that varies with depth, effective unit weight and pile diameter. In the present study, the recommendation provided by Rollins et al. (2005) is used in LPile analyses. An effective unit weight of 7 kN/m^3 is used for the loose liquefied sand layer. The soil below the liquefied layer is a dense sand, which is modeled based on the recommendation of Reese et al. (1974), with the following parameters: an effective unit weight of 10.19 kN/m^3, the initial modulus of subgrade reaction of 34 MPa/m, and an angle of internal friction of 45°.

The following properties are used for the steel pile: the modulus of elasticity of 210 GPa, a yield strength of 315 MPa, and Poisson's ratio of 0.23. The nominal moment capacity of the pile is 8,031 kN-m.

The pile is modelled as for a free-head condition. The force exerted by the sliding crust on the pile is calculated based on the FE analysis for two pile spacing presented above. The total maximum lateral reaction force F_0 = 1,030 kN and moment M_0 = 2,417 kN-m are obtained at the base of the 5-m rigid pile segment in the crust (i.e. at point B in

Fig. 2) for 3D pile spacing. Similarly, F_0 = 713 kN and M_0 = 1,892 kN-m are obtained for 2D pile spacing. In the LPile analysis, F_0 and M_0 are applied at the free-head.

Figure 6 shows the deflection, bending moment, and shear force in the pile for s = 2D and 3D. With an increase in pile spacing, the force on the pile due to crust movement increases, which results in a larger deflection of the pile. The magnitude of deflection decreases with depth, and is negligible ~10 m below the interface between the crust and liquefied layer (Fig. 6(a)). The maximum bending moment develops ~1.5 m below the interface between the liquefied loose sand and non-liquefied dense sand layers. Therefore, this section of the pile would have the largest possibility of damage. Note that, based on field observation, Cubrinovski et al. (2009) reported that the largest damage of piles due to the 1995 Kobe earthquake occurred slightly below the liquefied layer.

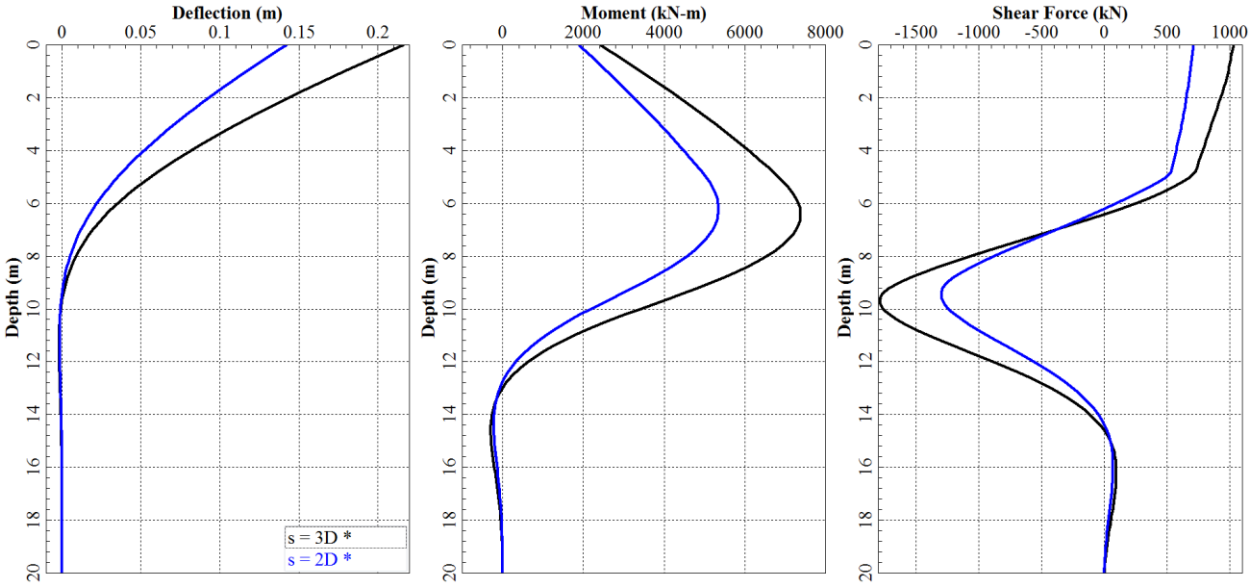

Figure 6: Structural response of pile for varying spacing

6 CONCLUSIONS

Numerical analyses are performed to investigate the response of piles subjected to passive loading resulting from lateral spreading due to an earthquake. First, three-dimensional finite-element (FE) analyses are performed for the displacement of a clay crust over a liquefied (weak) loose sand layer, which exerts a large lateral load on a row of piles. The analysis is performed using Abaqus/Explicit FE software. The calculated lateral force increases with pile spacing; however, for a pile spacing greater than five diameters ($s \geq 5D$), the spacing does not have a significant influence on lateral resistance, and the pile behaves as a single pile. For a given pile spacing, the lateral force increases with the undrained shear strength of clay (s_u); however, the normalized maximum lateral resistance is independent of s_u. The arching effect is significant for a pile spacing less than 2D. The soil flows between the piles for $s \geq 5D$. The LPile analyses show that the maximum bending moment generates at a location below the interface between the liquefied and stable layer, which represents a segment of possible damage.

In the FE analyses presented in this paper, the pile segment in the upper crust is modelled as a rigid body. FE analysis for the full length of the pile, considering its flexibility, might provide a better insight into the pile–soil interaction behaviour.

ACKNOWLEDGEMENTS

The work presented in this paper has been supported by the Natural Sciences and Engineering Research Council of Canada (NSERC), Petroleum Research Newfoundland and Labrador and Mitacs.

REFERENCES

ABAQUS 6.14 [Computer software]. D. S. Simulia, *Dassault Systémes*.

Bauer, J., Kempfert, H.G. and Reul, O. 2014. Lateral Pressure on Piles due to Horizontal Soil movement – 1g Model Tests on Single Piles and Pile Rows, 8th International Coference on Physical Modeling in Geotechnics, Perth, Australia, (2): 839–846.

Cai, F. and Ugai, K. 2000. Numerical analysis of the stability of a slope reinforced with piles, *Soils and Foundations*, 40(1): 73–84.

Cubrinovski, M., Ishihara, K. and Poulos, H. 2009. Pseudo-Static Analysis of Piles Subjected to Lateral Spreading, *Bulletin of the New Zealand Society for Earthquake Engineering*, 42(1): 28–38.

Hawlader, B., Dutta, S., Fouzder, A. and Zakeri, A. 2015. Penetration of Steel Catenary Riser in Soft Clay Seabed: Finite-Element and Finite-Volume Methods, *International Journal of Geomechanics, ASCE*, 15(6): 04015008. doi: 10.1061/(ASCE)GM.1943-5622.0000474.

Ito, T. and Matsui, T. 1975. Methods to estimate lateral force acting on stabilizing piles, Soils and Foundations, 15(4): 43–59.

Karmaker, R. and Hawlader, B. 2018. Modeling of Pile Stabilized Clay Slopes Using a Large Deformation Finite-Element Method, *7th Canadian Geohazards Conference,* Paper No-155.

Kokusho, T. 1999. Water Film in Liquefied Sand and Its Effect on Lateral Spread, *Journal of Geotechnical and Geoenvironmental Engineering*, 125(10): 817–826.

Kourkoulis, R., Gelagoti, F., Anastasopoulos, I. and Gazetas, G. 2012. Hybrid method for analysis and design of slope stabilizing piles, *Journal of Geotechnical and Geoenvironmental Engineering*, 137(1): 1–14.

Liu, L. and Dobry, R. 1995. Effect of Liquefaction on Lateral Response of Piles by Centrifuge Model Tests. *NCEER Bulletin*, 9(1): 7–11.

Matlock, H. 1970. Correlations for Design of Laterally Loaded Piles in Soft Clay, *2nd Offshore Technology Conference, Texas*, (I): 577–594.

McVay, M., Zhang, L., Molnit, T. and Lai, P. 1998. Centrifuge Testing of Large Laterally Loaded Pile Groups in Sands, *Journal of Geotechnical and Geoenvironmental Engineering*, 124(10): 1026–1026.

Randolph, M.F. and Houlsby, G.T. 1984. The Limiting Pressure on a Circular Pile Loaded Laterally in Cohesive Soil, *Géotechnique*, 34(4): 613–623.

Reese, L.C., Cox, W.R. and Koop, F.D. 1974. Analysis of Laterally Loaded Piles in Sand, *6th Offshore Technology Conference, Houston, Texas*, II: 473–484.

Rollins, K.M., Gerber, T.M., Lane, J.D. and Ashford, S.A. 2005. Lateral Resistance of a Full-Scale Pile Group in Liquefied Sand. Journal of the Geotechnical and Geoenvironmental Engineering Division, ASCE, 131: 115–125.

Taghavi, A., Muraleetharan, K.K., Miller, G.A. and Cerato, A.B. 2016. Centrifuge Modeling of Laterally Loaded Pile Groups in Improved Soft Clay, *Journal of Geotechnical and Geoenvironmental Engineering, ASCE*, 142(4): 04015099 doi: 10.1061/(ASCE) GT.1943-5606.0001443.

Wang, S.T., Vasquez, L. and Reese, L.C. 2008. Study of the Behavior of Pile Groups in Liquefied Soils, *14th World Conference on Earthquake Engineering, Beijing, China*.

Welch, R.C., and Reese, L.C. 1972. Laterally Loaded Behavior of Drilled Shafts, *Center for Highway Research Report, the University of Texas at Austin*, 3(5): 65–89.

Wilson, D.W. 1998. Soil-pile-Superstructure interaction in Liquefying Sand and Soft Clay, *Ph.D. Dissertation*, Department of Civil and Environmental Engineering, University of California, Davis.